Supporting Information

Catalytic effect of cytochrome c on H_2O_2 oxidation of a *p*-hydroxyphenyl-substituted BODIPY derivative

Qinhai Xu [a]*, Kang Li [b], Yang Liu [a], Delong Kong [a], Peng Wang [b]

[a] College of Chemistry, Chemical Engineering and Materials Science, Zaozhuang University, Zaozhuang 277160, Shandong Province, China

[b] School of Chemistry and Life Resources, Renmin University of China, Beijing 100872, China

* Corresponding author, E-mail address:1249661455@qq.com.

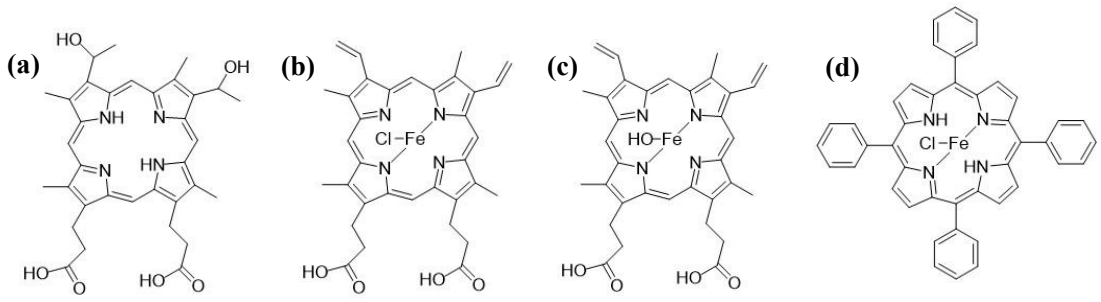

Figure S1. (a) Chemical structure of Hematoporphyrin (He). (b) Chemical structure of Hemin (Hc). (c) Chemical structure of Hematin porcine (Hh). (d) Chemical structure of Iron(IIII) Meso-Tetraphenylporphine Chloride (It).

S1.1. Reagents

2,4-dimethylpyrrole, 4-carboxybenzaldehyde, Trifluoroacetic acid (TFA), 2,3-Dichloro-5,6-dicyano-1,4-benzoquinone (DDQ), Triethylamine, Boron trifluoride diethyl etherate, *p*-hydroxybenzaldehyde, Acetic acid, Piperidine, Toluene, DMSO-d6, H_2O_2 (AR, 30 WT. % in H_2O) were purchased from Aladdin Industrial Corporation (Shanghai, China).

S1.2. Apparatus

The ^1H NMR and ^{13}C NMR spectra were examined using a Bruker 600 MHz instrument, and the chemical shifts were reported on the delta scale in ppm relative to DMSO-d6 (δ = 2.50 ppm) for ^1H NMR and DMSO-d6 (δ = 39.51 ppm) for ^{13}C NMR.

S1.3. Synthesis of BOH

A BODIPY derivative BOD was firstly synthesized following Safacan Kolemen's method [S1]. Then, BOD (2.5 mM, 0.92 g) and *p*-hydroxybenzaldehyde (7.5 mM, 0.92 g) were added to a 500 mL round-bottomed flask. 200 mL of toluene, 0.5 mL of piperidine and 0.5 mL of acetic acid were added into the solution. The mixture was heated under reflux using a Dean Stark trap. The reaction process was monitored by TLC ($CHCl_3$: MeOH = 97:3). The starting materials were consumed, the solution was cooled to room temperature and washed for three times with water. The organic phase was dried with anhydrous Na_2SO_4 and evaporated by using a rotary evaporator. The residue was purified through silica gel column chromatography using chloroform and methanol ($CHCl_3$: MeOH = 97:3) as the eluant. Purple black solid (BOH, 0.27 g, 23%) [S2]. BOH: ^1H NMR (600 MHz, DMSO-d6): δ_H 8.12 (d, J = 8.1 Hz, 2H), 7.54 (d, J = 7.8 Hz, 2H), 7.50 (s, 1H), 7.47 (d, J = 8.5 Hz, 2H), 7.32 (d, J = 16.3 Hz, 1H), 6.94 (s, 1H), 6.90 (d, J = 4.3 Hz, 2H), 6.18 (s, 1H), 2.49 (s, 3H), 1.39 (s, 3H), 1.34 (s, 3H). ^{13}C NMR (600 MHz, DMSO-d6): δ_C 167.35, 159.67, 154.30, 154.03, 142.87, 141.56, 39.06, 138.98, 138.54, 138.48, 132.26, 30.75, 130.52, 129.52, 129.07, 127.54, 121.59, 118.75, 116.54, 115.11, 55.25, 14.72, 14.39 ppm. QTOF-MS (m/z): $[M+H]^+$ calc'd for $C_{27}H_{24}BF_2N_2O_3$: 473.1843, Found: 473.1842, Δ=0.21 ppm [S3].

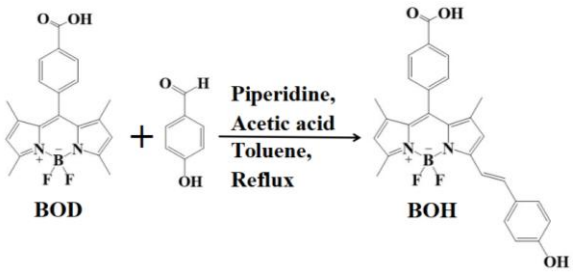

Figure S2. Synthesis of the *p*-hydroxystyryl-substituted BODIPY derivative (BOH).

[S1] Kolemen S., Bozdemir O., Cakmak Y.. Optimization of distyryl-Bodipy chromophores for efficient panchromatic sensitization in dye sensitized solar cells. Chem. Sci. 2011;2: 949–954.

[S2] Lu Y., Ke H., Wang Y., Zhang Y., Li H., Huang C., Jia N.. A ratiometric electrochemiluminescence resonance energy transfer platform based on novel dye BODIPY derivatives for sensitive detection of lactoferrin, Biosens. Bioelectron. 2020;170:112664.

[S3] Xu Q., Li K., Wang P.. The reaction mechanism of *p*-hydroxystyryl-substituted BODIPY with $ABTS^{\bullet+}$ and Fe^{3+} in solutions and in liposomes. Arab. J. Chem. 2025;18:106041.

S1.4. NMR spectrum and QTOF-MS spectrum of BOH

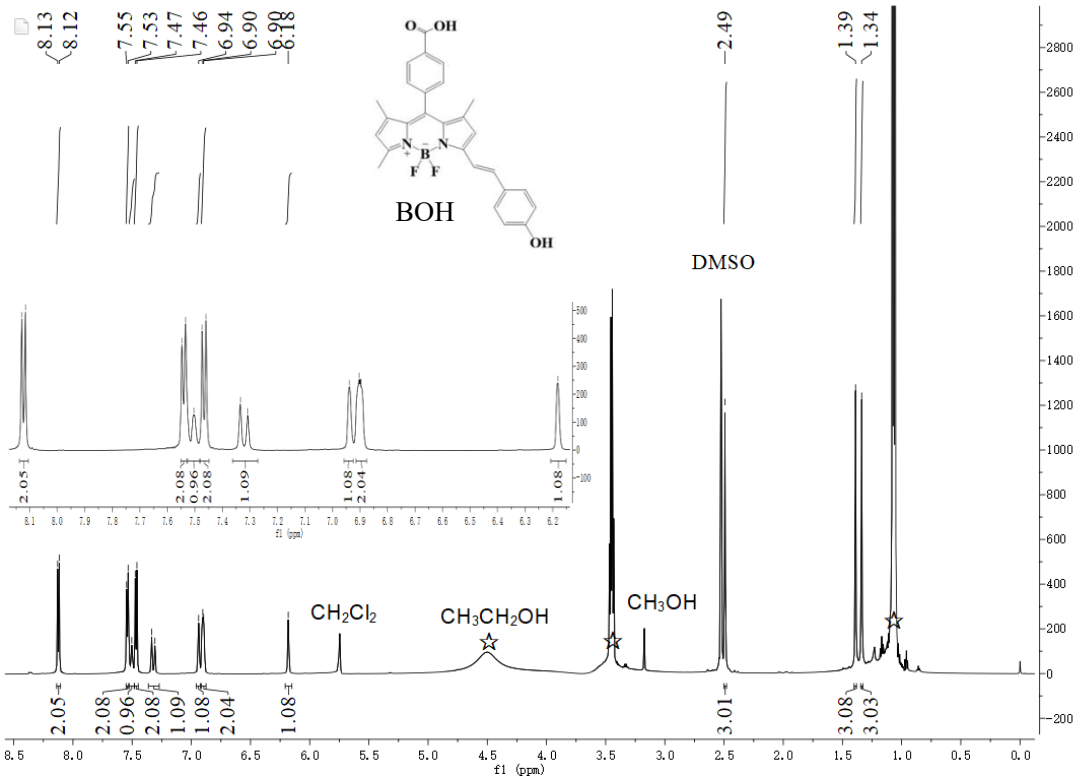

Figure S3. ^{1}H-NMR spectrum of BOH in $(CD_3)_2SO$.

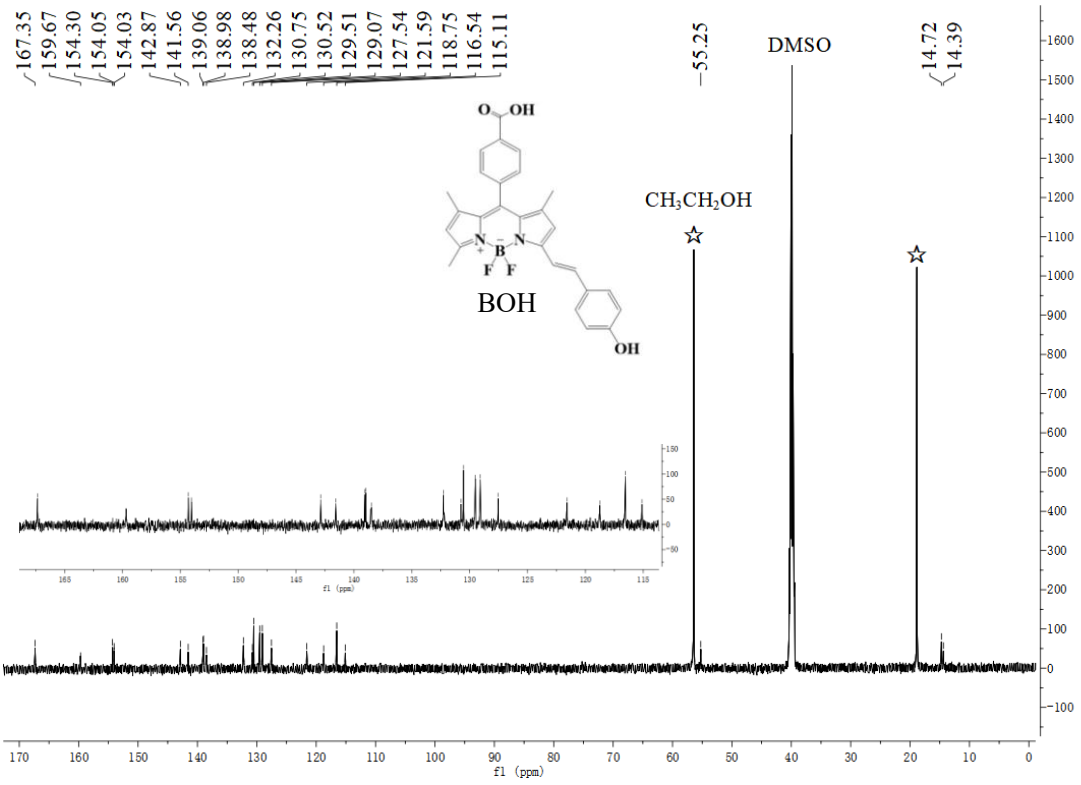

Figure S4. ^{13}C-NMR spectrum of BOH in $(CD_3)_2SO$.

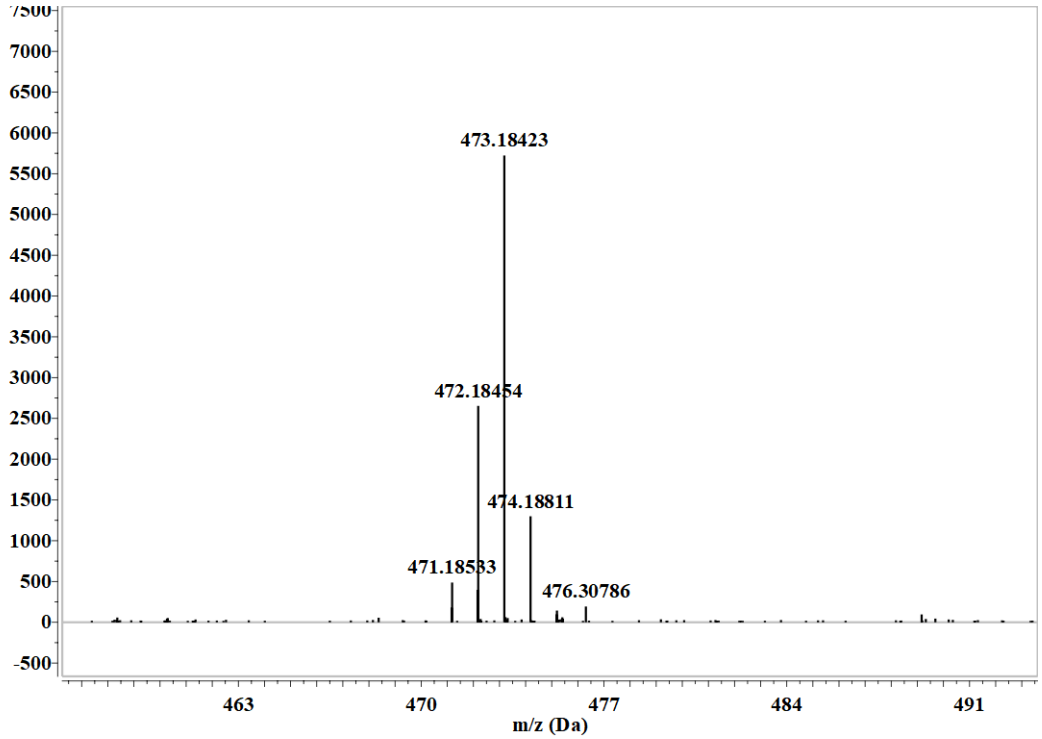

Figure S5. QTOF-MS spectrum of BOH.

S1.5. Characteristic spectra of BOD and BOH

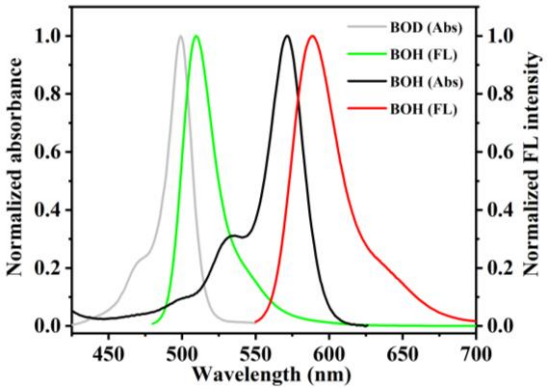

Figure S6. Normalized absorption spectra and fluorescence emission spectra (λ_{Ex} = 450 nm) of BOD in ethanol solution and normalized absorption spectra and fluorescence emission spectra (λ_{Ex} = 520 nm) of BOH in ethanol solution [S3].

The absorption peaks of BOD and BOH were observed at 499 nm and 572 nm in ethanol solution, respectively. The fluorescence emission peaks of BOD and BOH were observed at 509 nm and 589 nm in ethanol solution.

Table S1. Physicochemical parameters of BOH in ethanol solution [S3].

	ε/L·mol^{-1}cm^{-1}	λ_{max}^{Abs}/nm	λ_{max}^{Em}/nm	Φ_{FL}/%	τ_{FL}/ns	TEAC	Redox potential (V vs. RHE)	pKa	LogP$_{Cal}$
BOH	107758	572	589	79.90	4.08	1.31	0.17	4.19, 9.33	1.32

[S3] Xu Q., Li K., Wang P.. The reaction mechanism of *p*-hydroxystyryl-substituted BODIPY with ABTS$^{\bullet+}$ and Fe^{3+} in solutions and in liposomes. Arab. J. Chem. 2025;18:106041.

S1.6. Effect of BOH on Cyt-c

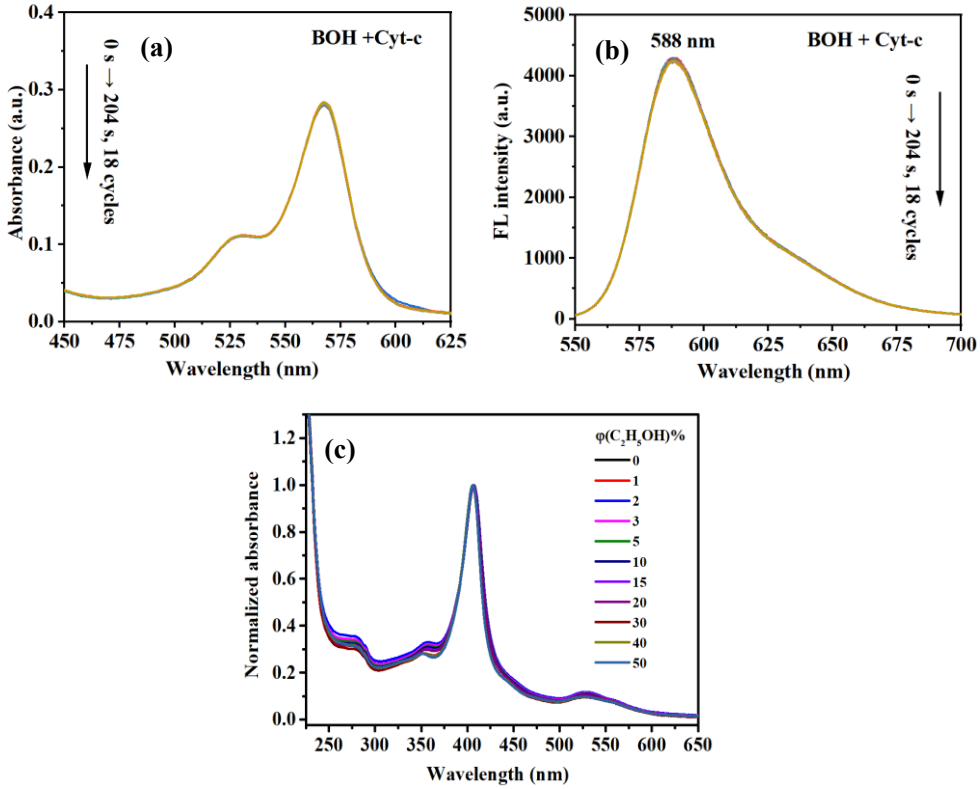

Figure S7. (a) The absorption spectra of BOH and Cyt-c within 18 cycles in 204s. (b) Fluorescence emission spectra of BOH and Cyt-c within 18 cycles in 204s. (c) Normalized absorption spectra of Cyt-c (10^{-5} M) with different volume ratio of ethanol to water.

The interaction between Cyt-c and BOH was investigated in this study. It demonstrated that the characteristic absorption and fluorescence emission peaks of BOH at 570 and 588 nm remained unchanged after the addition of Cyt-c, indicating the absence of any chemical reaction between BOH and Cyt-c (Figure S7a and S7b). To further understand the impact of ethanol on Cyt-c, which served as the solvent for the redox reaction of BOH + Cyt-c + H_2O_2, experiments were conducted using a mixture of ethanol and water. The absorption spectra revealed that the Soret band at 408 nm of Cyt-c exhibited minimal change as the percentage of ethanol increased, suggesting that ethanol had a negligible effect on the α-helix secondary structure of Cyt-c (Figure S7c) [S4]. The presence of a stable secondary structure of Cyt-c in the ethanol solvent was conducive to the oxidation of BOH by H_2O_2, which was catalyzed by Cyt-c.

[S4] Gong J., Yao P., Jin L., Jiang M., Chunyu L.. Conformational transition of cytochrome c and apocytochrome c induced by ethanol. Fudan Univ J Med Sci (Nat Sci) 2001;40:355–359. DOI:10.3969/j.issn.0427-7104.2001.04.002.

S1.7. The mass spectra of the catalysis of Cyt-c on the oxidation of BOH by H_2O_2

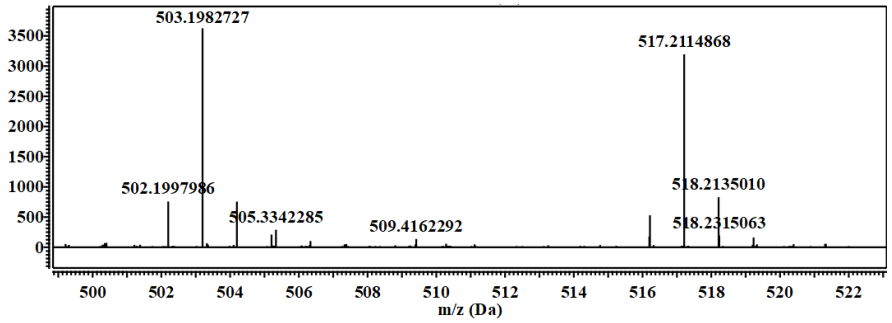

Figure S8. HPLC-QTOF-MS spectrum of BOD + Cyt-c + H_2O_2.

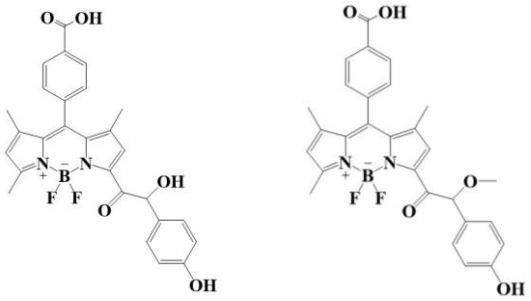

1h **2h**

1h: HPLC-QTOF-MS (m/z): $[M-H]^-$ calc'd for $C_{27}H_{22}BF_2N_2O_5$: 503.1595, Found: 503.1983

2h: HPLC-QTOF-MS (m/z): $[M-H]^-$ calc'd for $C_{28}H_{24}BF_2N_2O_5$: 517.1751, Found: 517.2115

S1.8. The catalysis of hemoproteins on the oxidation of BOH by H_2O_2

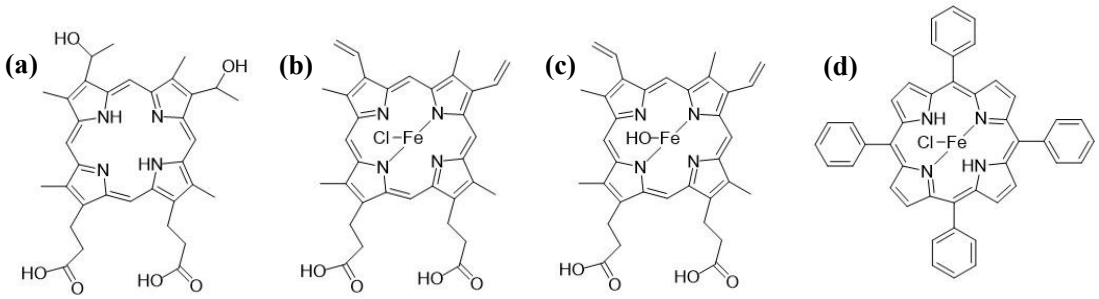

Figure S1. (a) Chemical structure of Hematoporphyrin (He). (b) Chemical structure of Hemin (Hc). (c) Chemical structure of Hematin porcine (Hh). (d) Chemical structure of Iron(IIII) Meso-Tetraphenylporphine Chloride (It).

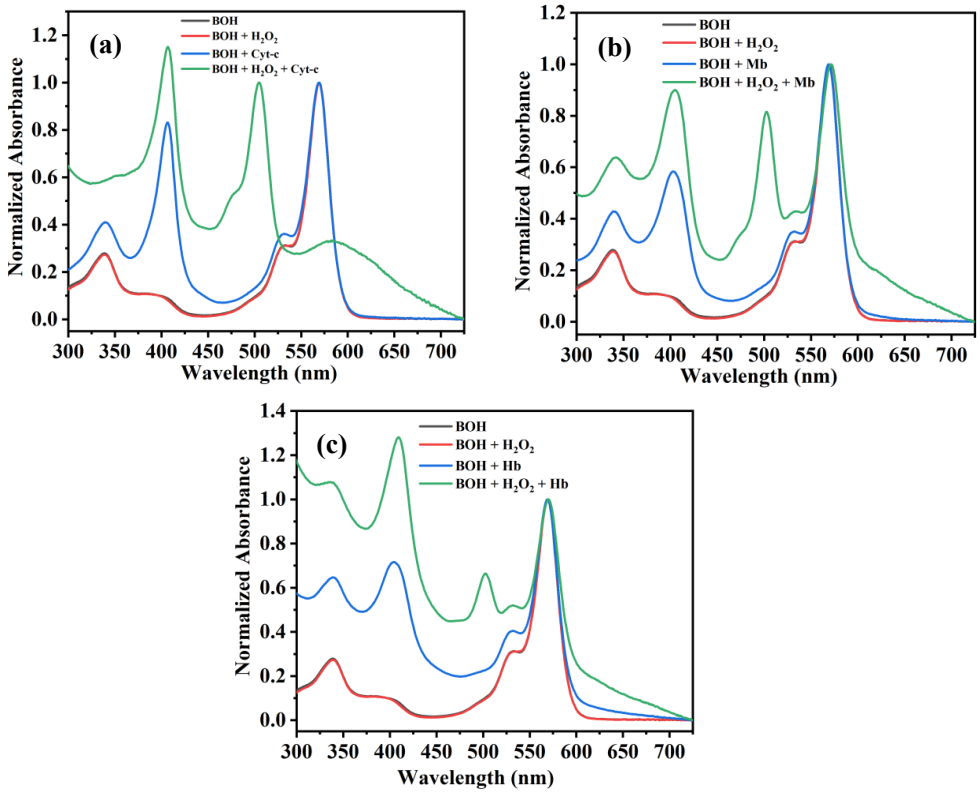

Figure S9. (a) The absorption spectra of BOH, BOH + H_2O_2, BOH + Cyt-c, and BOH + H_2O_2 + Cyt-c . (b) The absorption spectra of BOH, BOH + H_2O_2, BOH + Mb, and BOH + H_2O_2 + Mb. (c) The absorption spectra of BOH, BOH + H_2O_2, BOH + Hb, and BOH + H_2O_2 + Hb.

S1.9. Amino acid sequences of cytochrome c, myoglobin and hemoglobin

S1.9.1. Cytochrome c (Protein Data Bank entry 1HRC)

GDVEK GKKIF VQKCA QCHTV EKGGK HKTGP NLHGL FGRKT GQAPG FTYTD ANKNK GITWK EETLM EYLEN PKKYI PGTKM IFAGI KKKTE REDLI AYLKK ATNE HEC

S1.9.2. Myoglobin (Protein Data Bank entry 1WLA)

GLSDG EWQQV LNVWG KVEAD IAGHG QEVLI RLFTG HPETL EKFDK FKHLK TEAEM KASED LKKHG TVVLT ALGGI LKKKG HHEAE LKPLA QSHAT KHKIP IKYLE FISDA IIHVL HSKHP GDFGA DAQGA MTKAL ELFRN DIAAK YKELG FQG HEM SO4

S1.9.3. Hemoglobin (Protein Data Bank entry 2QSS)

VLSAA DKGNV KAAWG KVGGH AAEYG AEALE RMFLS FPTTK TYFPH FDLSH GSAQV KGHGA KVAAA LTKAV EHLDD LPGA SELSD LHAHK LRVDP VNFKL LSHSL LVTLA SHLPS DFTPA VHASL DKFLA NVSTV LTSKY RHEM CMO

MLTAE EKAAV TAFWG KVKVD EVGGE ALGRL LVVYP WTQRF FESFG DLSTA DAVMN NPKVK AHGKK VLDSF SNGMK HLDDL KGTFA ALSEL HCDKL HVDPE NFKLL GNVLV VVLAR NFGKE FTPVL QADFQ KVVAG VANAL AHRYH HEM CMO

VLSAA DKGNV KAAWG KVGGH AAEYG AEALE RMFLS FPTTK TYFPH FDLSH GSAQV KGHGA KVAAA LTKAV EHLDD LPGAL SELSD LHAHK LRVDP VNFKL LSHSL LVTLA SHLPS DFTPA VHASL DKFLA NVSTV LTSKY RHEM CMO

MLTAE EKAAV TAFWG KVKVD EVGGE ALGRL LVVYP WTQRF FESFG DLSTA DAVMN NPKVK AHGKK VLDSF SNGMK HLDDL KGTFA ALSEL HCDKL HVDPE NFKLL GNVLV VVLAR NFGKE FTPVL QADFQ KVVAG VANAL AHRYH HEM CMO

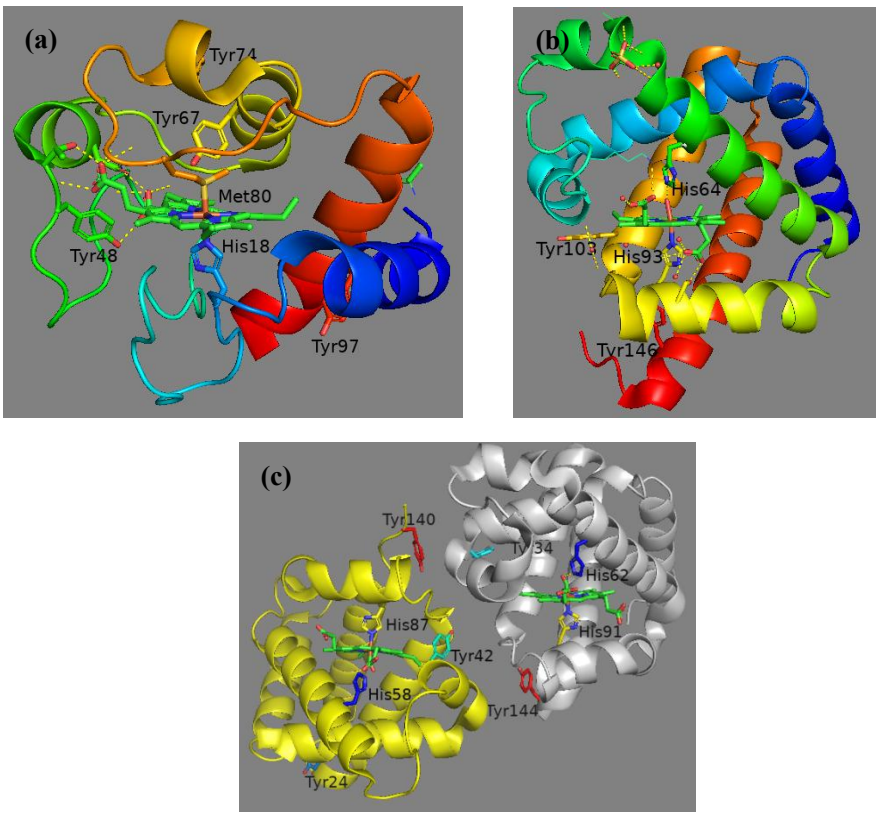

Figure S10. (a) Crystal structure of Cytochrome c (Protein Data Bankentry 1HRC). (b) Crystal structure of Myoglobin (Protein Data Bank entry 1WLA). (c) Crystal structure of Hemoglobin (Protein Data Bank entry 2QSS).

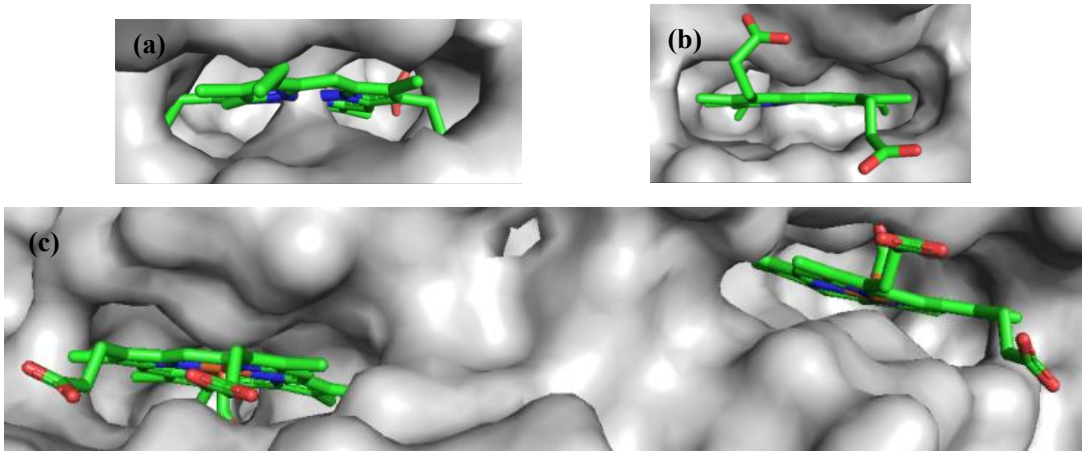

Figure S11. (a) Cytochrome c surface (Protein Data Bank entry 1HRC). (b) Myoglobin surface (Protein Data Bank entry 1WLA). (c) Hemoglobin surface (Protein Data Bank entry 2QSS).

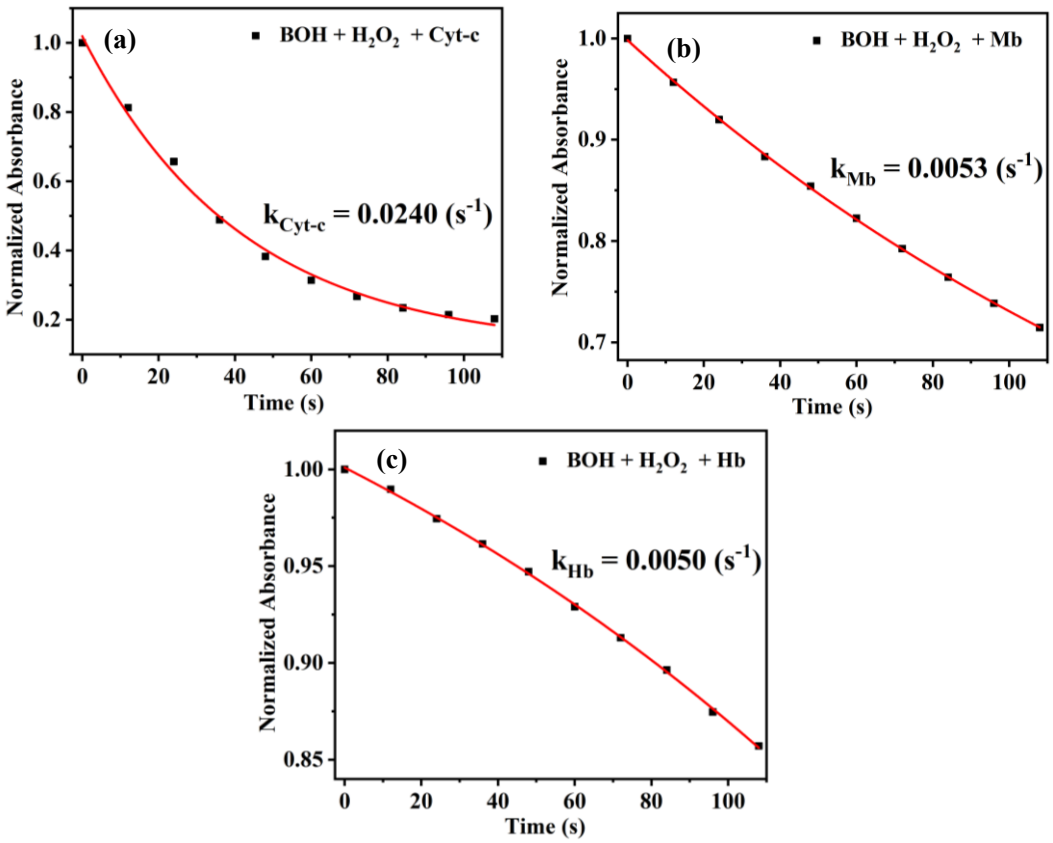

Figure S12. (a) Chemical kinetic of BOH + H_2O_2 + Cyt-c measured at 568 nm. (b) Chemical kinetic of BOH + H_2O_2 + Mb measured at 568 nm. (c) Chemical kinetic of BOH + H_2O_2 + Hb measured at 568 nm.